Magnetization measurements on frozen ferrofluids: an attempt to separate interaction and anisotropy influences

2006 J. Phys.: Condens. Matter 18 4921

(http://iopscience.iop.org/0953-8984/18/20/016)

INSTITUTE OF PHYSICS PUBLISHING JOURNAL OF PHYSICS: CONDENSED MATTER

J. Phys.: Condens. Matter **18** (2006) 4921–4934 doi:10.1088/0953-8984/18/20/016

Magnetization measurements on frozen ferrofluids: an attempt to separate interaction and anisotropy influences

O Michele, J Hesse and H Bremers

Institut für Metallphysik und Nukleare Festkörperphysik, Technische Universität, Mendelssohnstrasse 3, D-38106 Braunschweig, Germany

E-mail: h.bremers@tu-braunschweig.de

Received 3 February 2006, in final form 7 April 2006
Published 5 May 2006
Online at stacks.iop.org/JPhysCM/18/4921

Abstract

In this contribution we focus on a novel way to perform and evaluate magnetization experiments on frozen ferrofluids or magnetic nanoparticles fixed in space. The basic idea is to project the behaviour of a real particle system onto a Stoner–Wohlfarth (SW) particle ensemble behaviour. Therefore first an ideal SW particle system acting as a reference system with unique particle sizes and orientation of easy axis was studied numerically by introducing a particle–particle interaction via a demagnetizing field. We have shown that for non-interacting SW particles a universal mean value rule holds that the magnetization measured after ZFC (zero field cooling) can be expressed as a mean value of the magnetization measured after PHFC and NHFC (positive and negative high field cooling) processes. Any deviation from this mean value rule is therefore due to non-SW behaviour (multidirectional anisotropy and interaction) only and can be derived from the magnetization measurements and be compared with simulations.

By this new method it is possible to determine the mean value of the particle's anisotropy and the mean interaction which is expressed here as a magnetic field.

We will report on experiments performed on frozen ferrofluids because these systems offer the possibility of complete thermal demagnetization after melting. In this contribution we describe experiments performed on two different frozen Co-based ferrofluids by SQUID magnetometry.

1. Introduction

Nanomagnetism is part of nanophysics, which is a real and exciting field of applied and basic research nowadays. In the last decades great progress has been achieved in understanding the

physical properties of magnetic nanoparticle systems. The problem is quite complex because each individual particle exhibits a magnetic moment and an anisotropy energy characterized by one or more easy axes. In a real particle system the particle–particle interaction is an additional parameter which depends on the vicinal spatial arrangement of the particles in the system. The problem to describe the properties of a particle system becomes more complex because in a real system there is unavoidably a particle size distribution, a distribution of particle distances and a distribution of the particle easy axes orientation. Considering a system of typical 10^6 to 10^9 single domain nanoparticles, any information about interaction and anisotropy must have the character of a mean value being characteristic for the whole ensemble.

In this introduction the progress achieved until now will be briefly presented by citing some typical papers as examples: the first attempt to consider the magnetism of a nanoparticle system in terms of the well known superparamagnetism normally described by the Langevin function fails. The particle's intrinsic anisotropy 'destroys' this well known magnetic behaviour as experimentally demonstrated by Williams *et al* [1]. Recently Wickhorst *et al* [2] discussed this problem using the term 'anisotropic superparamagnetism'.

The influence of particle–particle interactions was evidenced many years ago by experiments of Weili *et al* [3] and still is a challenge in its theoretical description [4, 5]. Monte Carlo computer simulation reveals deeper insight in the connection of the local physical processes experienced by each particle and as a consequence the resulting behaviour of the whole system, as recently presented by Chantrell *et al* [6] who calculated the susceptibility of nanoparticle systems. The particle–particle interaction has been attacked and described many times [4, 5].

Dormann *et al* [7] discussed models for interparticle interactions. Very early, Dormann *et al* [8] considered superparamagnetism versus spin-glass laws. A very interesting detail is the investigation of spin-glass properties in such nanoparticle systems because when assuming dipole–dipole interaction both conditions for spin-glass behaviour are present: competing interactions and site disorder [9]. The dipole–dipole interaction is treated in recent papers by Hansen *et al* [10] and El-Hilo *et al* [4]

In real nanoparticle systems the particle's surface also plays an important role, as reported by Tronc *et al* [11]. These effects also influence the superparamagnetic relaxation, discussed by Mørup *et al* [12]. In this contribution the blocking temperature is calculated in the presence of weak interactions. A review of models describing the dynamics of interacting particles was presented by Hansen and Mørup [13].

Mössbauer spectrometry is a microscopic tool with a limited timescale. Mørup [14] was the first who paid attention to this fact and calculated the expected average value of the magnetic hyperfine field observed in such spectra. Due to collective magnetic excitation causing fluctuations of the hyperfine field that are fast in comparison to the Mössbauer time scale, the observed splitting is smaller than it would be in the absence of fluctuations. Recently an alternative approach for the interpretation of the observed spectra and line shapes was proposed [15, 16].

The physical basis of nanomagnetism was given many years before the world-wide activities started. Two publications should be mentioned here. First Stoner and Wohlfarth [17] presented a basic contribution explaining the observed high coercivity values in some ferromagnetic alloys by properties of embedded single domain particles. At nearly the same time Néel [18] contributed fundamental ideas to explain the magnetic properties of small particles with the advantage of considering thermal activated magnetization fluctuations over particle inherent anisotropy energy barriers. In the more then 50 intermediate years since the appearance of both these fundamental papers a lot of effort and success in the understanding of magnetic properties of single domain particle systems has been achieved.

We are interested in the investigation of the magnetic properties of nanoparticle systems from the basic physical point of view. Instead of the very popular consideration of the magnetization versus applied external magnetic field (hysteresis measurements) we prefer the consideration of the magnetization versus temperature, applying a constant magnetic field. As has been recently reported [20], by considering magnetization measurements after well defined processes of reaching the low-temperature magnetic state it is possible to apply new strategies in performing magnetization experiments when measuring the magnetization versus temperature. Using these strategies we discovered that the SW model bears a generally valid mean value rule which allows one to define a deviation resulting from the difference in the behaviour of a real particle system in comparison with the ideal SW particle system.

The aim of this contribution is to derive information about the particle–particle interactions and anisotropy in nanosized magnetic single domain particle systems in which the particles are fixed in space. The work presented here is based on experiments performed on frozen ferrofluids and on very basic calculations using the ideal picture of SW particles together with thermally activated changes in the particle system magnetization.

2. Basic considerations

All considerations are based on the Stoner–Wohlfarth [17] model for single domain magnetic particles. This model bears the particles' anisotropy energy as an intrinsic property. It is rather easy to extend this model following the ideas of Néel [18] by introducing thermally driven magnetization fluctuations in the particles because the SW model represents a two-level system. The energy density E for one particle fixed in space with given orientation of the easy axis reads

$$E(\phi, \theta, B_{\text{ext}}, K, M_0) = -M_0 \cdot B_{\text{ext}} \cos\phi - K \cdot \cos^2(\phi - \theta). \tag{1}$$

The equilibrium position of the particle's magnetization vector is described by the angle ϕ. It depends on four additional parameters: the angle θ between the easy axis and the external magnetic field B_{ext}, the anisotropy constant K, and the saturation magnetization M_0 of the material from which K and M_0 represent intrinsic properties of the particles in question.

It should be mentioned that the SW model neglects the fact that each magnetic moment (also the very big ones of magnetic nanoparticles) is inevitably connected with a torque. Therefore each change of the magnetic moment spatial position is to be assumed as infinitely fast. In reality this 'switching behaviour' must be considered as a dynamic process, for example by solving the Landau–Lifshitz–Gilbert equation [22]. The magnetization reversal by uniform rotation was treated by Wernsdorfer *et al* [23]. The magnetization switching for small ferromagnetic particles in a Heisenberg model was presented by Hinzke and Nowak [24].

In 'static' considerations, normally a characteristic switching field B_{Switch} is considered, which is defined as the field strength to which only one minimum of the energy density corresponds.

$$\frac{\mathrm{d}E}{\mathrm{d}\phi} = 0 \qquad \text{and} \qquad \frac{\mathrm{d}^2E}{\mathrm{d}\phi^2} = 0. \tag{2}$$

$$B_{\text{switch}} = \frac{2K}{M_0}\left(\cos^{2/3}\theta + \sin^{2/3}\theta\right)^{-3/2}. \tag{3}$$

This kind of calculation was performed by [25–27] using these relations. Deviations from the SW relation can be seen in the so-called Henkel plot, which neglects any thermal activation. The so-calculated switching field is independent of the particle size (volume), and this fact

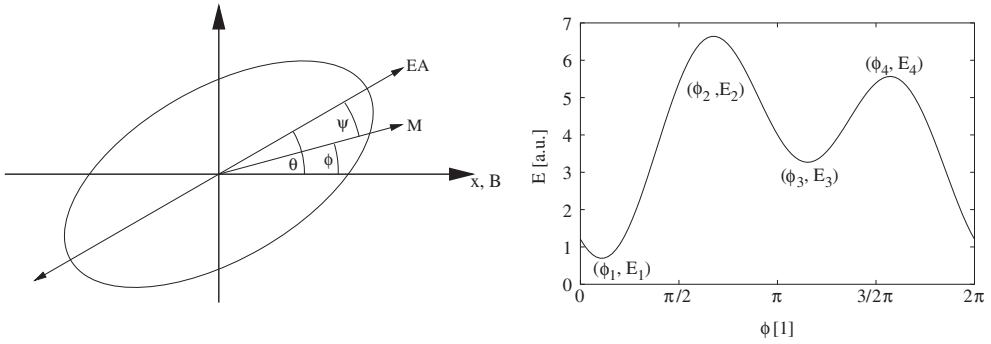

Figure 1. Left: equilibrium magnetization for one SW particle fixed in space. An external magnetic field B is applied along the x-axis. The easy axis (EA) is indicated. All angles are defined in the figure. Right: the energy density E plotted versus the angle for the above introduced SW particle in an external magnetic field not exceeding the switching field strength.

contradicts the experiment. To describe real experimental results the change from one particle to a particle system must be done first. An extension of the SW model (like the classical work of Néel) must be considered which bears in mind that the SW model is a two-level system. Allowing thermally induced jumps of the particle's magnetization from one energy minimum (=level) to the other (see figure 1), a basic relaxation equation for the particle ensemble's magnetization $M(t)$ can be found.

$$\frac{\mathrm{d}M(t)}{\mathrm{d}t} = \beta(B_{\mathrm{ext}}, T, \nu_0) \cdot \left(M_{\mathrm{equi}} - M(t)\right). \tag{4}$$

Here M_{equi} means the normalized equilibrium magnetization of the particle system. When the system consists of N particles per volume unit and each particle exhibits a magnetic moment of $\mu = M_0 \cdot V$, the system magnetization is normalized to $N \cdot \mu$. The relaxation rate is expressed by $\beta(B_{\mathrm{ext}}, T, \nu_0)$ and consists of four terms:

$$\beta(B, T, \nu_0) = \nu_0 \left(p_{13}^{(1)} + p_{13}^{(2)} + p_{31}^{(1)} + p_{31}^{(2)}\right).$$

These describe the probability for 'jumps' of the magnetization vector from the minimum energy E_2 to the energy levels E_1, and E_3 and also from the minimum energy E_4 to the energy levels E_1, and E_3 in agreement with figure 1. Two of these terms are given as examples.

$$p_{13}^{(1)} = \exp\left(\frac{E_2 - E_1}{k_B T}\right)$$

$$p_{13}^{(2)} = \exp\left(\frac{E_4 - E_1}{k_B T}\right).$$

ν_0 is the so-called anlauf frequency, being a characteristic constant for the nanoparticles in question (typical order 10^9 to 10^{11} s^{-1}). It is a very important fact that the relaxation rate (or time) in the interaction-free SW model only depends on temperature T and the external field B_{ext}, and is independent of the initial state of the magnetization [21].

3. Interacting Stoner–Wohlfarth particles

In a recent paper, Michele *et al* [20] summarized many experimental ways to prepare well defined low-temperature magnetic states of a nanoparticle system. From that, three processes

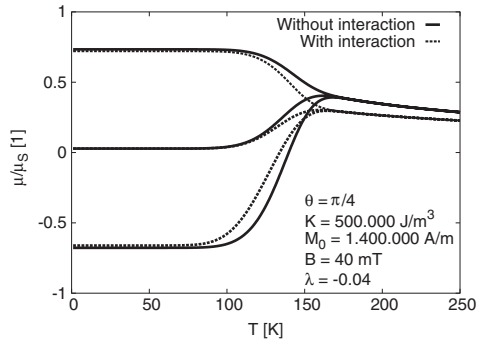

Figure 2. Result of calculation for the magnetization after PHFC, ZFC and NHFC in the case of non-interacting particles ($\lambda = 0$) and interacting particles ($\lambda = -0.04$).

are important for this contribution: zero field cooling (ZFC), positive high field cooling (PHFC) and negative high field cooling (NHFC). High field means that the field strength exceeds the switching field for all particles in the system. From such well defined low-temperature magnetization states the magnetization measurement starts applying an external (weak) magnetic field and increasing the temperature by a constant heating rate.

The starting conditions for solving the relaxation equation (4) after the three different cooling procedures ZFC, PHFC and NHFC are

$$M_{\mathrm{PHFC}//\mathrm{FW}}(0) = 1; \qquad M_{\mathrm{NHFC}//\mathrm{FW}}(0) = -1; \qquad M_{\mathrm{ZFC}//\mathrm{FW}}(0) = 0. \quad (5)$$

Using these starting conditions, the relaxation equation can be solved. This has been done numerically for a system of non-interacting identical particles being fixed in space first. The angle $\theta = \frac{\pi}{4}$ with respect to the applied external magnetic field was chosen. The saturation magnetization $M_0 = 1.4 \times 10^6$ A m^{-1} and the anisotropy energy density $K = 4.0 \times 10^5$ J m^{-3} were assumed for the numerical calculations. The results are presented in figure 2.

The easiest way to introduce interaction is to use the molecular field ansatz. In the following the external magnetic field B_{ext} in the interaction-free SW model (see above) is replaced by B_{int}:

$$B_{\mathrm{int}}(t) = B_{\mathrm{ext}} + \lambda \cdot M(t) \quad (6)$$

where λ represents a phenomenological interaction parameter like the demagnetizing field for ferromagnetic samples with finite size and defined shape.

The introduction of the interaction changes the relaxation rate. The course of the three magnetizations when starting from the low-temperature magnetic state after PHFC, ZFC and NHFC are different from the corresponding curves without interaction. An example of such calculation results is also shown in figure 2.

Now a very important feature of the SW model is introduced. For a non-interacting SW particle system the mean value relation

$$M_{\mathrm{ZFC}//\mathrm{FW}}(T) = \tfrac{1}{2}\left(M_{\mathrm{PHFC}//\mathrm{FW}}(T) + M_{\mathrm{NHFC}//\mathrm{FW}}(T)\right) \quad (7)$$

always holds, as shown by Michele *et al* [20, 21]. This fact is used here to define first a normalized temperature dependent difference $\widetilde{\Delta}(T)$, which is non-zero when interaction is present.

$$\widetilde{\Delta}(T) = \frac{M_{\mathrm{ZFC}//\mathrm{FW}}(T) - M_{\mathrm{calc.}}(T)}{M_{\mathrm{ZFC}//\mathrm{FW}}(T)}. \quad (8)$$

M_{calc} is the mean of the upper PHFC and lower NHFC magnetization curves. In the second step we introduced a temperature-independent integral difference

$$\Delta = \int_0^{T_{\max}} \frac{M_{\mathrm{ZFC//FW}}(T) - M_{\mathrm{calc.}}(T)}{M_{\mathrm{ZFC//FW}}(T)}\,\mathrm{d}T. \tag{9}$$

$T_{\max}$ must be chosen at least as equal to the temperature where the three magnetization curves starting after PHFC, NHFC and ZFC become indistinguishable. In the ideal SW model this is the case when the temperature is high enough to overcome the magnetization blocking in the particles. To distinguish the results for $\widetilde{\Delta}(T)$ and Δ obtained from experiments we named them concisely as $\widetilde{\Delta}(T) =$ deviation and $\Delta =$ integral deviation.

4. Simulations

With the above-defined normalized temperature-dependent difference $\widetilde{\Delta}(T)$ (deviation) and the normalized integral difference Δ (integral deviation) systematic numerical studies have been performed considering different external magnetic fields, different particle sizes (magnetic moments), different anisotropy energy densities, different interaction parameter values and different orientations of easy axis expressed by Θ.

Investigating the influence of the particle size numerically, a very interesting exponential law with an introduced phenomenological parameter B_{decay} describing the dependence of the integral deviation from the external magnetic field was found:

$$\Delta(B) = \Delta(B = 0) \cdot \exp\left(-\frac{B_{\mathrm{ext}}}{B_{\mathrm{decay}}}\right). \tag{10}$$

The surprizing result is that the parameter B_{decay} is nearly independent of the particles' sizes. Therefore the parameter B_{decay} will also maintain its value in a real particle system where a size distribution is present. In contrast, the $\Delta(B = 0)$ value was found to be proportional to the particle volume.

Also, the influence of the anisotropy energy density represented by K was investigated numerically in the same manner. Some results are presented in figure 5. The results imply that B_{decay} is proportional to K and $\Delta(B = 0)$ is nearly independent of K.

Next the influence of the interaction parameter λ was investigated. The result in figure 6 shows that there is a simple proportionality between $\Delta(B = 0)$ and λ for not too big interaction parameter λ.

These above-mentioned facts allow the separation of the interaction energy from the anisotropy energy density influences on the magnetization of nanosized particle systems. First, a series of magnetization measurements after ZFC, PHFC and NHFC in weak external magnetic fields has to be performed. From these measurements $\widetilde{\Delta}(T, B_{\mathrm{ext}})$ must be determined, and from these values $\Delta(B_{\mathrm{ext}})$ is obtained. Plotting $\Delta(B_{\mathrm{ext}})$ in a logarithmic scale, both parameters $\Delta(B = 0)$ and B_{decay} are obtained. To calculate the K- and λ-values it is necessary to know the particle size distribution or at least the mean particle size. For ferrofluids these values are easily obtained by transmission electron microscopy (TEM) or room-temperature magnetization measurements. Next, it is necessary to choose an SW particle system as a reference. If we choose the SW system with data presented in figures 3–6, it is possible to assign the real particle system to the chosen SW system with interaction and so to determine the parameters K and λ.

5. Experimental details

We present examples of experiments (magnetization measurements) and their evaluations performed on two different cobalt ferrofluids. These ferrofluids are characterized by a log-

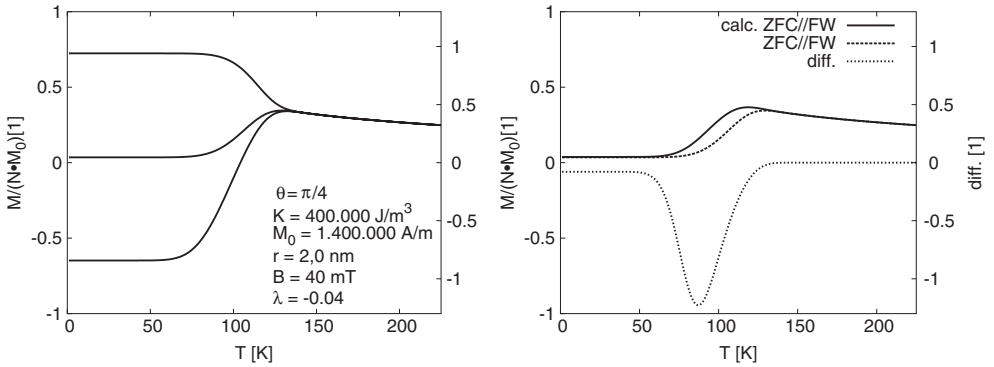

Figure 3. The normalized temperature-dependent difference $\widetilde{\Delta}(T)$ (right figure) as calculated from the magnetizations starting from a low-temperature magnetic state after ZFC, PHFC and NHFC (left figure).

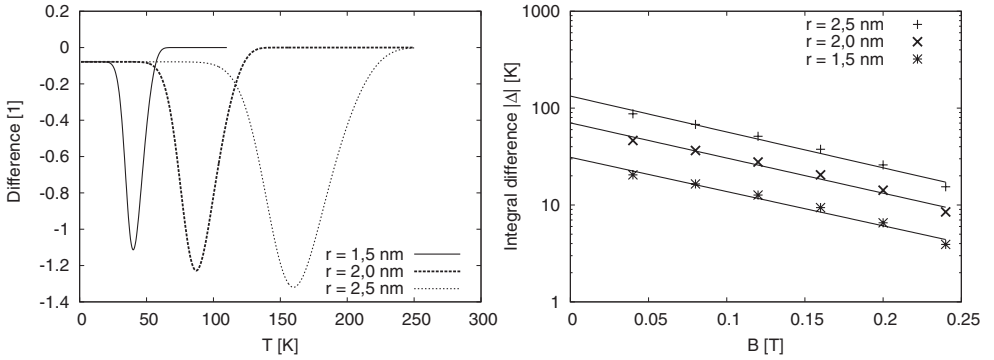

Figure 4. The left-hand part shows examples of the difference $\widetilde{\Delta}(T)$ for three different particle sizes (radius). In the right-hand part the exponential law describing the dependence of the normalized integral difference on the external magnetic field is shown.

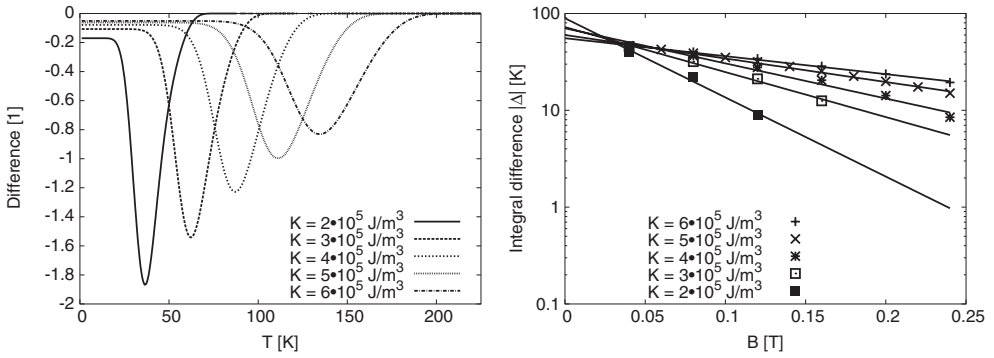

Figure 5. The left-hand part shows examples of the difference $\widetilde{\Delta}(T)$ for five particle anisotropy energy densities K. In the right-hand part the dependence of the integral difference on K is shown.

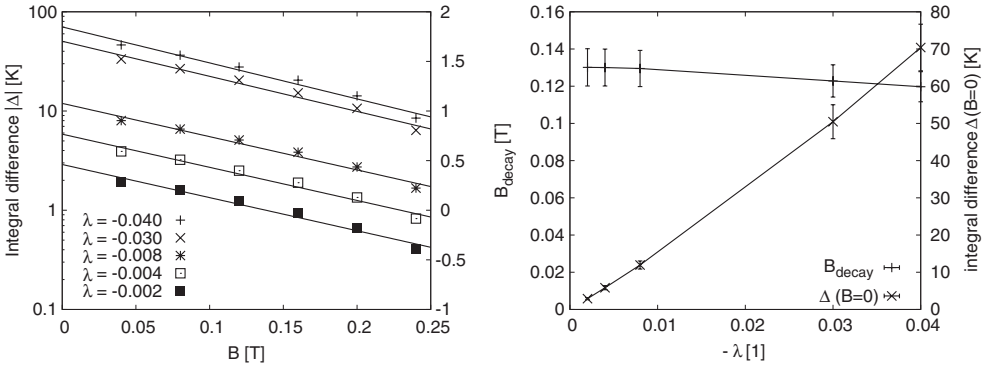

Figure 6. The normalized integral difference versus external magnetic field (left) and the relationship between ($B = 0$) and the interaction parameter λ (right).

normal particle radius distribution with the mean radius $\overline{r}$ and a standard deviation σ, the mean particle magnetic moment μ and the mean particle distance d. These data were gained from magnetization measurements at 300 K and a fit by a set of Langevin functions as described in detail in [19, 20]. Additional TEM was performed on dried samples. The solvent of the ferrofluids S was different, and its mean melting temperature (which in fact is a temperature range) is abbreviated by T_m. The properties of the Berlin Heart sample are $\overline{r} = 3.7$ nm, $\sigma = 0.6$ nm, $S =$ petroleum, $T_m = 150$ K. $\mu = 12\,400\ \mu_{Bohr}$, $d = 29$ nm. The properties of the University of Bielefeld sample are $\overline{r} = 1.63$ nm, $\sigma = 0.46$ nm, $S =$ orthodichlorbenzol, $T_m = 260$ K. $\mu = 2630\ \mu_{Bohr}$, $d = 40$ nm. So the second sample consists of much smaller particles than the first one.

As described in detail in [20] and also shown in figure 2, for each sample the well defined low-temperature magnetic states after PHFC, NHFC (the high field strength was 2 T) and ZFC were prepared before starting the magnetization measurements during warming up the sample in the weak external magnetic field. In performing these magnetization measurements we applied a heating rate of 3 K min^{-1}. The temperature T_{max} in all our measurements is well below the melting temperature of the solvent. Therefore we exclude particle rotation in the solvent as a process which also can contribute to the temperature dependence of the magnetization.

In figure 7 examples of measurements on the Berlin Heart ferrofluid after ZFC, PHFC and NHFC are shown. On the left-hand side a comparison of the mean magnetization after PHFC and NHFC (named calc. ZFC) with the magnetization measured after ZFC is shown. From these two curves the temperature-dependent deviation is calculated (right-hand part of figure 7), leading to the deviations plotted in figure 8. For each external field the integral deviation can be calculated. These values are plotted in a logarithmic scale in figure 9. An exponential law is fitted to this points to obtain the values $\Delta(B = 0)$ and B_{decay}. Comparing these values with the simulations led for the first sample to values of $K = 2 \times 10^5$ J m^{-3} for the anisotropy energy density and $\lambda = -0.0017$.

In figure 9 the value of the integral deviation corresponding to the measurement at the lowest external magnetic field value of 3 mT deviates from the straight line. Our measurement technique applied needs first a high magnetic field (we applied 2 T) for the PHFC or NHFC process. After that, the high field is switched to the low-field value. In the SQUID magnetometer this causes some residual magnetic flux in the superconducting coils which makes the low-field value unreliable. Therefore in all forthcoming measurements the very low magnetic fields are omitted and all measurements start with at least 10 mT.

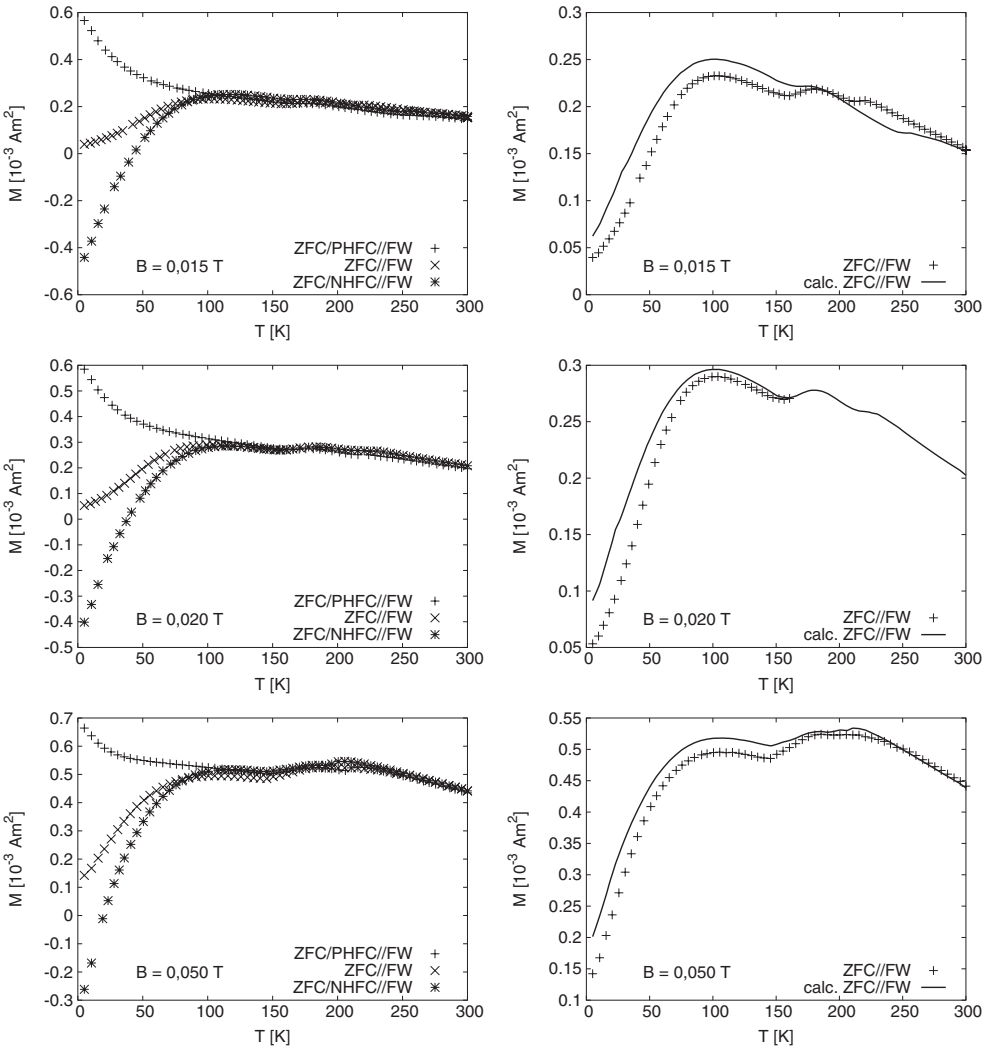

Figure 7. Examples of measurements after ZFC, PHFC and NHFC on the frozen Berlin Heart Coferrofluid (left-hand side). On the right-hand side the calculated mean value of the magnetization after PHFC and NHFC (solid line) and the magnetization after ZFC (crosses) is shown.

For the second sample (University of Bielefeld) the same way of evaluation led to $K = 1 \times 10^5$ J m^{-3} and $\lambda = 0.03$ (figures 10–12). In this case the λ-value is positive, representing an interaction field enhancing the magnetization between the particles. It must be mentioned that the simulations were made separately for the positive and negative values of λ.

The different signs of the λ-value give rise to the discussion of the interaction mechanism in the samples. The particles have very different sizes and therefore magnetic moments. In addition the concentration of the ferrofluids is different, and therefore the mean distances between the particles differ in the two samples. The stray field of bigger particles is of course much greater and therefore the interaction length not only ranges from particle to particle but possibly over a distance of many particles. The experiment shows that this results in a negative mean interaction field in the first sample (Berlin Heart). In the second sample (University of

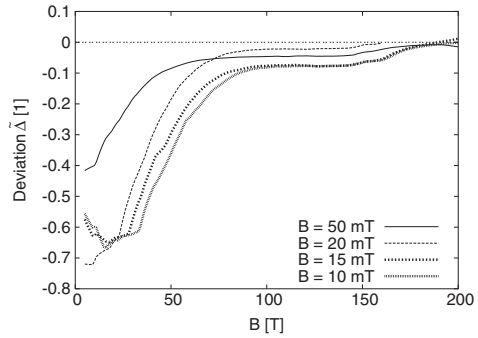

Figure 8. Temperature-dependent deviation $\widetilde{\Delta}(T)$ derived from the measurements presented in figure 7.

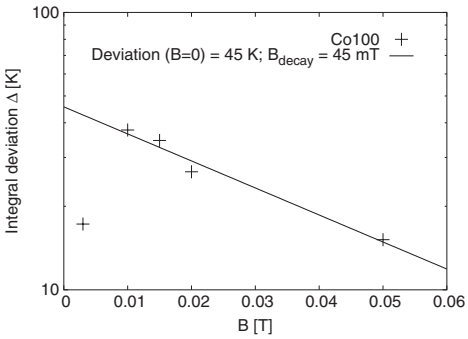

Figure 9. Integral deviation Δ derived from the values presented in figure 8. The straight line fits the parameters $\Delta(B = 0) = 45$ K and $B_{\text{decay}} = 45$ mT. The point at 3 mT deviating from the straight line is commented on in the text.

Bielefeld) the particle–particle interaction results in a positive mean interaction field. This rather surprising result may be caused by very small particles not to be seen in the TEM investigations. Their existence can be followed from the lack of saturation magnetization at 5 K until external fields of 5 T. Nevertheless the role of the particle surfaces (interfaces) can also lead to such effects. This remains a question that is open for further investigations. Also, we will not discuss here the possible collective behaviour of magnetic nanoparticles due to their interaction. In a recent paper [20] we presented conditions and experimental evidence for such effects and discussed for example the formation of dimers.

6. Summary and discussion

In this contribution, the Stoner–Wohlfarth model was the basis of our considerations and measurement evaluation. We succeeded in the characterization of real magnetic nanoparticle systems built by frozen ferrofluids and were able to characterize them by an interaction and anisotropy energy in the sense of characteristic mean values. This was possible by comparing magnetization measurement results after preparing well defined low-temperature magnetic states (PHFC and NHFC) before starting the field warming measurements performed in different weak external fields. For a non-interacting SW particle system the mean value relation (7) always holds. The violation of this rule allows the definition and evaluation of

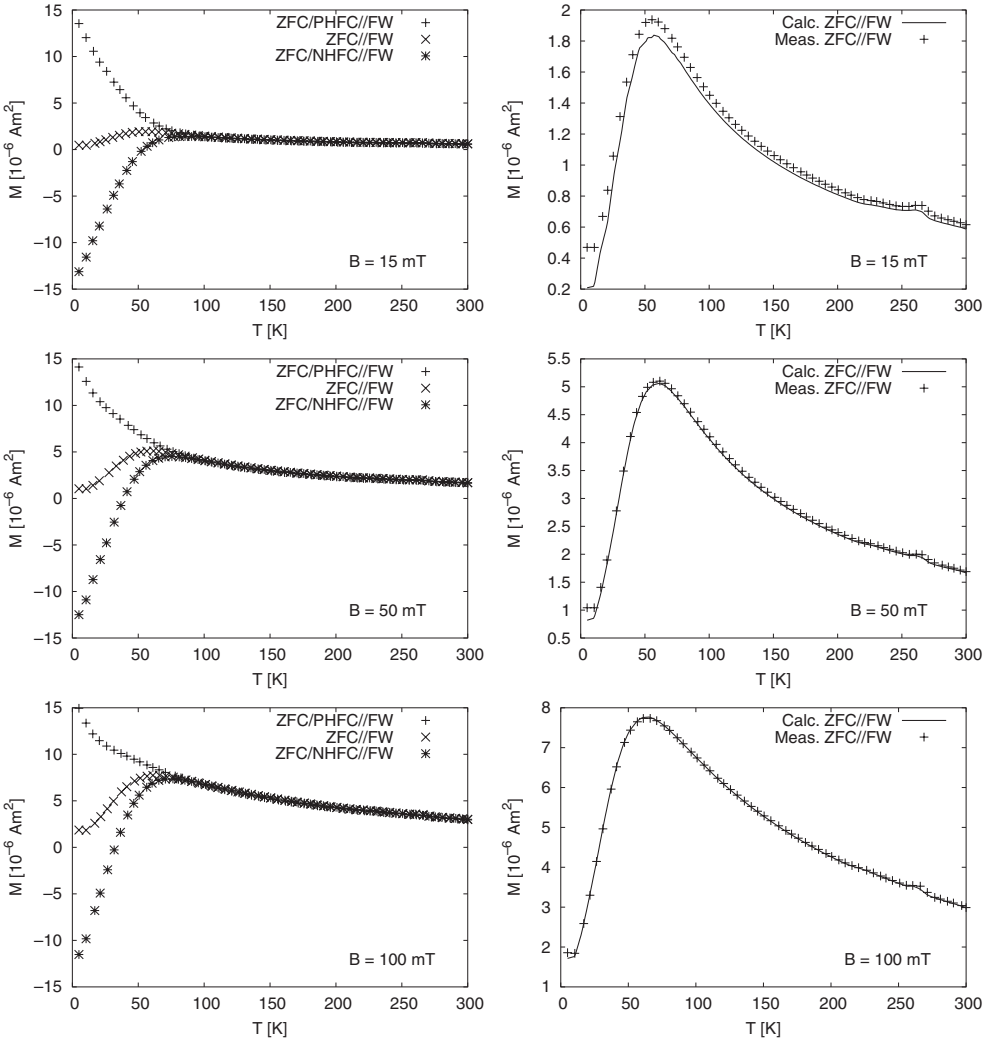

Figure 10. Examples of measurements after ZFC, PHFC and NHFC on the frozen Co-ferrofluid from the University of Bielefeld (left side). On the right-hand side the calculated mean value of the magnetization after PHFC and NHFC (solid line) and the magnetization after ZFC (crosses) is shown.

the deviation and the integral deviation for each applied external magnetic field. The decay law (10) was found by numerical calculations for the deviation. This new result allows the separation of influences of anisotropy and interaction. To obtain anisotropy and interaction values characteristic for the real system under consideration it was necessary to define an SW particle system to act as reference. For our evaluations we have chosen a completely textured ideal SW system with identical particles being fixed in space with the angle $\theta = \frac{\pi}{4}$ with respect to the applied external magnetic field. The saturation magnetization $M_0 = 1.4 \times 10^6$ A m^{-1} and the anisotropy energy density $K = 4.0 \times 10^5$ J m^{-3} were assumed for the magnetic material from which the particles were made.

Our research was directed towards basic physics using the idea of deviations from ideal SW behaviour. Therefore we summarize briefly the history of the deviations since the publication

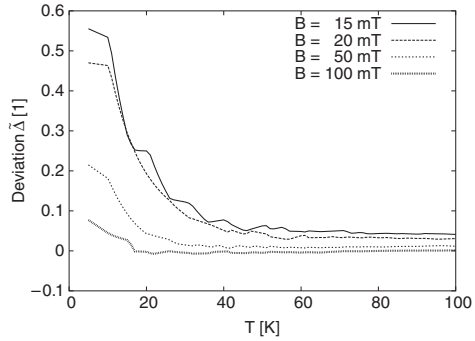

Figure 11. The temperature-dependent deviation $\widetilde{\Delta}(T)$ derived from the measurements presented in figure 10.

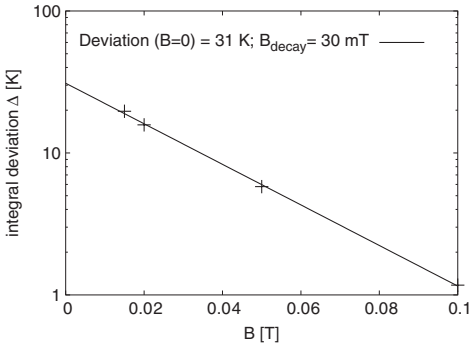

Figure 12. Integral deviation Δ derived from the values presented in figure 11. The straight line fits the parameters $\Delta(B = 0) = 31$ K and $B_{\mathrm{decay}} = 0.030$ T.

of the first fundamental SW paper [17]. This paper reports the simple and very characteristic property of SW particles in three-dimensional systems: the remanent magnetization is one half of the saturation magnetization. Wohlfarth [28] showed that for non-interacting single domain particles with uniaxial anisotropy, M_{r} (isothermal remanent magnetization) and M_{d} (DC demagnetized magnetization) are related for all applied external magnetic fields B according to

$$m_{\mathrm{d}}(B) = 1 - 2m_{\mathrm{r}}(B) \tag{11}$$

with

$$m_{\mathrm{d}} = \frac{M_{\mathrm{d}}}{M_0}; \qquad m_{\mathrm{r}} = \frac{M_{\mathrm{r}}}{M_0}. \tag{12}$$

Henkel [27] used this relation extensively and created the widely used Henkel plot. In subsequent papers [29] the following relation was applied:

$$\Delta m(B) = m_{\mathrm{d}}(B) - [1 - 2m_{\mathrm{r}}(B)]. \tag{13}$$

Mayo *et al* [30] introduced a so-called interaction-based deviation parameter, and Thamm and Hesse [25] related this parameter to the mean value of the upper and lower branches of the hysteresis loop and to the initial magnetization curve:

$$\Delta m(B) = m_{\mathrm{Initial}}(B) - \tfrac{1}{2}[m_{\mathrm{Upper}}(B) + m_{\mathrm{Lower}}(B)] \tag{14}$$

simplifying markedly the measurement time necessary for the Henkel plot. Also the proposed Thamm–Hesse plot presents $\Delta m(B)$ versus B, which gives a better insight in the meaning of the deviation when comparing with the Henkel plot, which hides the field dependence.

In a recent paper, Rellinghaus *et al* [31] reported magnetization measurements performed on FePt nanoparticles. They extensively used the Henkel plot and called the deviation $\Delta m(B)$ in formula (13) an 'interaction-based deviation'. In most cases this deviation may indicate interactions, but being very strict it must be mentioned that this deviation also is non-zero when a magnetic nanoparticle system is absolutely interaction free but exhibits multiaxial anisotropy [25]. Therefore it is still a challenge to separate the influences of anisotropy and interactions. One proposal to do this is presented in this paper. On the other hand our contribution shows the power of the highly idealized SW model and its contribution to the basic physical understanding of the magnetic properties of nanoparticle systems.

Acknowledgments

Our thanks go to Dr K Weyand and H Ahlers, Physikalisch-Technische Bundesanstalt, Braunschweig, for allowing us access to the SQUID magnetometer facility in their laboratory. We are grateful to Dr C Gansau and Dr N Buske from Mediaport Kardiotechnik GmbH in Berlin for supplying us with their ferrofluids. It is a great pleasure also to acknowledge the fruitful collaboration with Professor Dr A Hütten, Daniela Sudfeld, Inga Ennen and K Wojczykowski from the University of Bielefeld for the preparation of excellent ferrofluid samples and their electron microscopic characterization.

References

[1] Williams H D, O' Grady K and El Hilo M 1993 *J. Magn. Magn. Mater.* **122** 129–33
[2] Wickhorst F, Shevchenko E, Weller H and Kötzler J 2003 *Phys. Rev.* B **67** 224416
[3] Luo W, Nagel S R, Rosenbaum T F and Rosensweig R E 1991 *Phys. Rev. Lett.* **67** 2721
[4] El-Hilo M, Shatnawy M and Al-Rsheed A 2000 *J. Magn. Magn. Mater.* **221** 137
[5] Vieira S R, Nobre F D and da Costa F A 2000 *J. Magn. Magn. Mater.* **210** 390–402
[6] Chantrell R W, Walmsley N, Gore J and Maylin M 2000 *Phys. Rev.* B **63** 024410
[7] Dormann J L, Fiorani D and Tronc E 1999 *J. Magn. Magn. Mater.* **202** 251–67
[8] Dormann J L, Bessais L and Fiorani D 1988 *J. Phys. C: Solid State Phys.* **21** 2015–34
[9] Kleemann W, Petracic O, Binek Ch, Kakazei G N, Pogorelov Yu G, Sousa J B, Cardoso S and Freitas P P 2001 *Phys. Rev.* B **63** 134423
[10] Hansen M F, Jönsson P E, Nordblad P and Svedlindh P 2002 *J. Phys.: Condens. Matter* **14** 4901
[11] Tronc E, Ezzir A, Chekaoui R, Chanéac C, Nougés M, Kachkachi H, Fiorani D, Testa A M, Grenèche J M and Jolivet J P 2000 *J. Magn. Magn. Mater.* **221** 63–79
[12] Mørup S and Tronc E 1994 *Phys. Rev. Lett.* **72** 3278–81
[13] Hansen M F and Mørup S 1998 *J. Magn. Magn. Mater.* **184** 262–74
[14] Mørup S 1983 *J. Magn. Magn. Mater.* **37** 39–50
[15] Afanas'ev A M and Chuev M A 2001 *JETP Lett.* **74** 107–10
[16] Chuev M A, Hupe O, Afanas'ev A M, Bremers H and Hesse J 2002 *JETP Lett.* **76** 558–62
[17] Stoner E C and Wohlfarth E P 1948 *Phil. Trans. R. Soc.* A **240** 599
Stoner E C and Wohlfarth E P 1991 *IEEE Trans. Magn.* **27** 3475
[18] Luis Néel M 1949 *Ann. Géophys.* **5** 99–136
[19] Weser T and Stierstadt K 1985 *Z. Phys.* B **59** 253–6
[20] Michele O, Hesse J, Bremers H, Polychroniadis E K, Efthimiadis K G and Ahlers H 2004 *J. Phys.: Condens. Matter* **16** 427–43
[21] Michele O 2004 *PhD Thesis* Technische Universität Braunschweig (http://opus.tu-bs.de/opus/volltexte/2005/646 Papierflieger Verlag GmbH Clausthal-Zellerfeld ISBN 3-89720-736-2 (2004))
[22] Bauer M, Fassbender J, Hillebrands B and Stamps R L 2000 *Phys. Rev.* B **61** 3410
[23] Wernsdorfer W, Thirion C, Demoncy N, Pascard H and Mailly D 2002 *J. Magn. Magn. Mater.* **242–245** 132

[24] Hinzke D and Nowak U 1998 *Phys. Rev.* B **58** 265
[25] Thamm S and Hesse J 1996 *J. Magn. Magn. Mater.* **154** 254–62
[26] Thamm S and Hesse J 1998 *J. Magn. Magn. Mater.* **184** 245–55
[27] Henkel O 1962 *Phys. Status Solidi* **2** 78
Henkel O 1962 *Phys. Status Solidi* **2** 1393
Henkel O 1964 *Phys. Status Solidi* **7** 919
[28] Wohlfarth E P 1958 *J. Appl. Phys.* **29** 595
[29] Kelly P E, O'Grady K, Mayo P I and Chantrell R W 1989 *IEEE Trans. Magn.* **25** 3881
[30] Mayo P I, O'Grady K, Kelly P I, Cambridge J, Sanders I L, Yogi T and Chantrell R W 1991 *J. Appl. Phys.* **69** 4733
[31] Rellinghaus B, Stappert S, Acet M and Wassermann E 2003 *J. Magn. Magn. Mater.* **266** 142–54